Temperature-dependent diffusing acoustic wave spectroscopy with resonant scatterers

Valentin Leroy and Arnaud Derode
Laboratoire Ondes et Acoustique, Université Paris Diderot-Paris 7, ESPCI-CNRS (UMR 7587), 10 rue Vauquelin, 75005 Paris, France
(Received 15 October 2007; published 5 March 2008)

The influence of a slight temperature change on the correlation of multiply scattered acoustic waves is studied, and experimental results are discussed. The technique presented here, similar to diffusing-acoustic-wave spectroscopy, is based on the sensitivity of a multiply scattering medium to a slight change. Ultrasonic waves around 3 MHz are transmitted through a sample made of steel rods in water and recorded by an array of transducers at different temperatures. The cross correlations between highly scattered signals are computed. The main effect of the temperature change is a simple dilation of the times of arrival, due to a change of the sound velocity in water. But the scatterers also play a role in the progressive decorrelation of wave forms. An analysis resolved in both time and frequency shows that at some particular frequencies, the resonant behavior of the scatterers is responsible for a significantly larger decorrelation. Interestingly, the experimental results allow one to detect the presence of a small resonance that was not detected earlier on the same scatterers with classical measurement of the scattering mean free path. A simple model is proposed to interpret the experimental results.

DOI: 10.1103/PhysRevE.77.036602 PACS number(s): 43.35.+d, 43.20.+g, 43.90.+v

I. INTRODUCTION

The propagation of a wave—whatever its physical nature—in a strongly scattering medium gives rise to complicated, randomlike wave forms. As the order of scattering grows, the measured wave forms become more and more sensitive to a slight perturbation of the medium. This can be a disadvantage for applications such as telecommunications which require the propagation channel to remain stable during the transmission. Yet one can also exploit the sensitivity of multiply scattered waves to quantify the change. This is the core of techniques known as diffusing-wave spectroscopy in optics [1,2], coda-wave interferometry [3–5], or the "doublet method" [6,7] in seismology or diffusing acoustic wave spectroscopy [8–10] in acoustics. Usually the perturbation of the medium is due to the movement of scatterers (e.g., particles in a suspension, bubbles in a liquid, etc.). In acoustics, detectors measure the wave field itself (amplitude and phase), which makes it possible to estimate directly the field-field correlation function and monitor the progressive decorrelation as the change in the medium becomes stronger.

In this paper, we consider a particular situation: the scattering structure does not move, but its temperature changes [11–14]. The evolution of scattered field is probed with ultrasonic waves in the MHz range. This is similar to diffusing acoustic wave spectroscopy (DAWS), except that the scatterers are fixed and the sound velocities are affected by the temperature change. We will study the field-field time correlation of multiply scattered waves (coda) in an open medium before and after a slight temperature change and, particularly, its dependence on time and frequency.

On the one hand, this question is closely related to time-reversal experiments in a changing environment [15–20]. Indeed, because of reciprocity, the field that is recreated at the source by a time-reversal device is directly proportional to the time autocorrelation of the scattered waves. If the medium has been perturbed before the wave is actually sent backward, the focusing amplitude will be degraded by a certain amount which is related to the degree of correlation between scattered waves before and after the perturbation. The amount of perturbation required to make the correlation drop by, say, 50% is a measurement of the sensitivity of the propagation medium to a particular change. This parameter is crucial for all applications of time-reversal focusing in real environments (acoustic waves in the ocean, microwaves for indoor communication, etc.). It is also analogous to the notion of fidelity (Loschmidt echo) in quantum physics [21].

On the other hand, aside from its connection with time-reversal, the sensitivity to a perturbation can be used as a tool to characterize a complex medium. For example, DAWS techniques were successfully applied to characterizing particle dynamics in fluidized suspensions [8], to distinguish between ballistic and random motions of scatterers in a reverberant cavity [22], or to reveal the degree of ray chaos in a solid block undergoing a temperature change [13]. In the experimental situation we consider here, ultrasonic waves are transmitted through a slab containing resonant scatterers which will be shown to exhibit an increased sensitivity around a particular resonance frequency that was not revealed by other measurements of transport parameters (mean free paths, diffusion constant).

II. EXPERIMENTAL PROCEDURE

The experiment was carried out in a large tank of water which was heated to a temperature of $T=25\ ^{\circ}\mathrm{C}$. Then, as the water was cooling down, acquisitions of multiply scattering signals were performed using the experimental setup depicted in Fig. 1. A subwavelength piezoelectric element transmitted a short ultrasonic pulse (three cycles of a 3-MHz sine wave) that propagated through water and encountered a sample made of a random collection of vertical steel rods, with a density of 18.75 cm^{-2} and a diameter of 0.8 mm (for comparison, the average wavelength in water was 0.47 mm). In the 2.4–4-MHz frequency range, the elastic mean free path ℓ_e of the scattering medium changes with frequency and

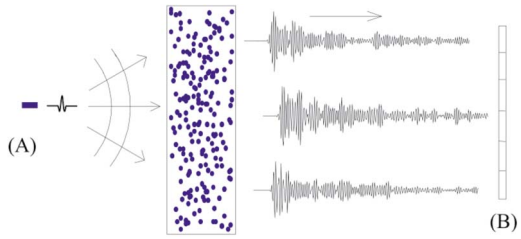

FIG. 1. (Color online) Sketch of the experimental setup. The source (a) emits a short pulse that propagates through the slab. The scattered waves are recorded on a 128-element array (b). The temperature is monitored by three PT-100 probes (not shown).

was found to vary between 3 and 7 mm [23,24]. Experimentally, the maximum value was attained around 2.7 MHz, which corresponded to a resonance of the rods. In this range of frequency, the sample thickness ($L=40$ mm) was much larger than the mean free path. As a consequence, the wave underwent strong multiple scattering as it traversed the sample. The multiply scattered pressure field emerging from the sample was recorded on the 128 subwavelength elements of the receiving array. An average over 50 emissions was performed to enhance the signal-to-noise ratio. The temperature of the water was monitored in different locations by three PT100 probes which measured temperature changes with a 0.02 °C accuracy. Within this accuracy, the temperature was homogeneous in the body of water and constant over the 50 emissions. Note that the vertical dimensions of the rods, the emitter, and the array were sufficiently large, compared to the wavelength, to consider the setup as two dimensional.

Let us denote $h_i(t)$ the reference signal, at $T=25$ °C, recorded on element i at time t. An example of such a signal, for $i=64$, is shown in Fig. 2(a). While the duration of the emitted pulse was 1 μs, the measured wave form showed a very long coda that spread over more than 350 μs, which is typical of multiple scattering. One of the main parameters of a multiply scattering sample is its diffusion time (proportional to the Thouless time). The ensemble averaged intensity $\langle h^2(t)\rangle = I(t)$ is often referred to as the "time-of-flight distribution" for the intensity [25,26]. In a slab with thickness L, when the diffusion approximation holds ($L \gg \ell_e$, $ct \gg \ell_e$), analytic expressions can be established: $I(t)$ obeys a diffusion equation (with the appropriate boundary conditions), and shows at late times an exponential decay with a typical time $t_D \sim L^2/\pi^2 D$. Here the diffusion constant D can be very roughly estimated by $D=\frac{1}{2}c\ell_e \sim 3.75$ mm$^2/\mu$s, hence $t_D \sim 40$ μs. This approximate value is consistent with the experimental observations: after the maximum, the decay time of the squared envelope of the coda, averaged on the 128 receivers, is 45 μs [see Fig. 2(b)]. Note that this comparison is very crude: intrinsic absorption has been ignored, as well as the frequency dependence of the diffusion constant and possible localization effects at late times [27]. Yet the order of magnitude is in fairly good agreement with the experimental decay time. If the diffusion approximation is not valid, more complex approaches involving solutions of the radiative transfer equation may be required [25,28]. From a

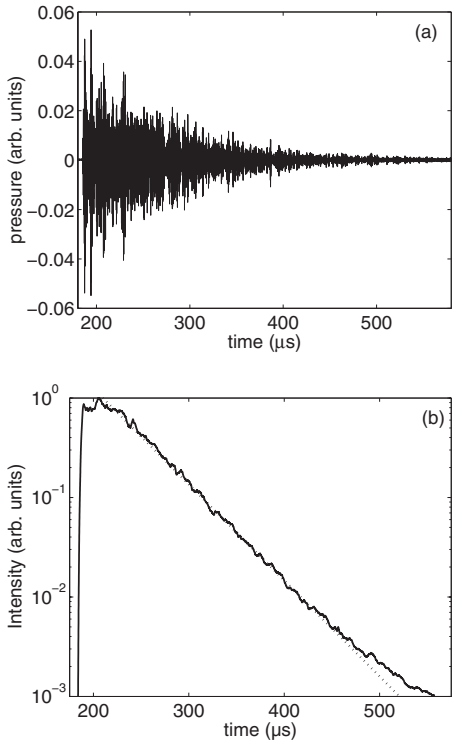

FIG. 2. (a) The pressure field recorded by the central element of the array ($i=64$) for the reference temperature $T=25$ °C. The time origin corresponds to the incident pulse emission. (b) Normalized mean intensity of the scattered signals as a function of time (log scale). Between 250 μs and 500 μs, the decay of the intensity is nearly exponential with a characteristic time $\tau_D \sim 45$ μs (straight dotted line).

physical point of view, the typical decay time τ_D of $I(t)$ depends on the sample thickness, its mean free path, and the wave speed. Another way to quantify the duration of $I(t)$ is to calculate the length of the time interval around the maximum to capture, e.g., 50% or 90% of the total energy in the coda. The experimental measurements yield $\Delta\tau_{50}=42$ μs and $\Delta\tau_{90}=120$ μs, and the maximum value of $I(t)$ occurs at $\tau_M=206$ μs (i.e., 19 μs after the ballistic time).

As the temperature decreases to $T-\Delta T$, the new signal is denoted $h_i^{\Delta T}(t)$. The effect of a temperature decrease is illustrated in Fig. 3, which displays a comparison between the reference signal and that obtained for $\Delta T=0.2$ °C on two different time windows. The wave that propagated in colder water looks like a time-delayed version of the reference wave. Furthermore, the delay is increasing with the arrival time, as the shift in Fig. 3(b) is larger than in Fig. 3(a). A more quantitative investigation consists in computing correlation functions. Let us denote $h(t;\tau,\Delta\tau)$ the reference signal, taken on time window $[\tau, \tau+\Delta\tau]$, and consider its correlation with $h^{\Delta T}(t)$:

$$g(t) = \sum_{i=1}^{128} \int d\theta\, h_i(\theta;\tau,\Delta\tau) h_i^{\Delta T}(\theta + t). \qquad (1)$$

The cross-correlation function $g(t)$ exhibits a peak at time δt, which gives an estimate of the time delay between the two

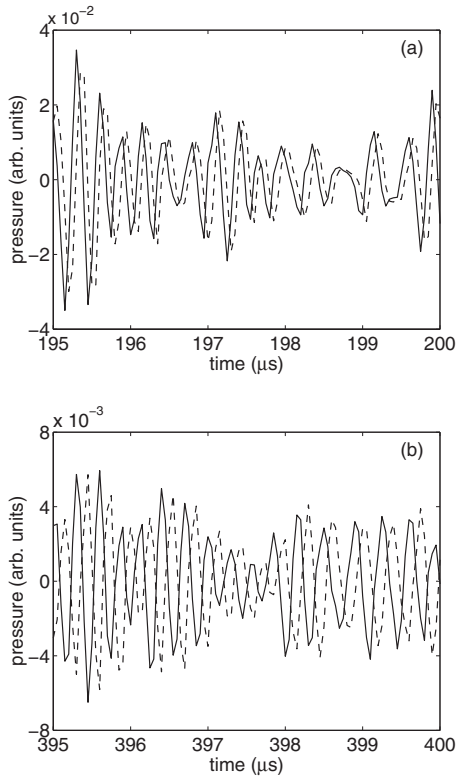

FIG. 3. Close-up of two parts of Fig. 2 (solid lines) and comparison with the signal acquired on the same array element for a temperature decrease of 0.2 °C (dashed lines). (a) Early times. (b) Later times. The signals are very similar, except for a global time translation, which is larger for later times.

signals. As an example, Fig. 4 shows $g(t)$ calculated for the 395–400 μs window drawn in Fig. 3(b). In this case, the peak of correlation is found at $\delta t=0.13$ μs, indicating that the decrease of 0.2 °C in temperature made the signal arrive 0.13 μs later. However, the effect of the temperature change is not a pure time shift: the signal is also slightly distorted. A measurement of this distortion is given by the amplitude of correlation G_i, estimated by comparing the $[\tau,\tau+\Delta\tau]$ window of h_i with the $[\tau+\delta t,\tau+\delta t+\Delta\tau]$ window of $h_i^{\Delta T}$:

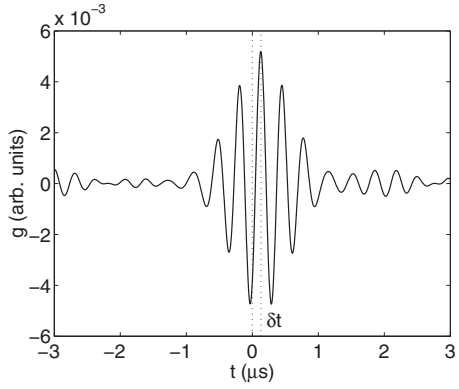

FIG. 4. The cross-correlation function of Eq. (1) calculated for the two signals shown in Fig. 3(b). The maximum occurs for $\delta t=0.13$ μs.

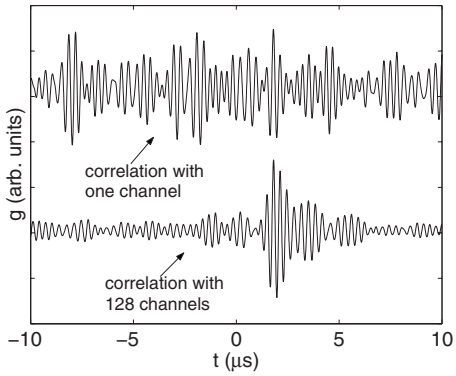

FIG. 5. The correlation function for a $\Delta T=2$ °C decrease is calculated on a time window $\Delta\tau=5$ μs wide centered at $\tau=300$ μs, with only one channel (upper plot) and with averaging over the 128 channels (lower plot).

$$G_i=\frac{\int dt\, h_i(t;\tau,\Delta\tau)h_i^{\Delta T}(t+\delta t;\tau+\delta t,\Delta\tau)}{\left\{\int dt[h_i(t;\tau,\Delta\tau)]^2\int dt[h_i^{\Delta T}(t+\delta t;\tau+\delta t,\Delta\tau)]^2\right\}^{1/2}}. \tag{2}$$

In the example of Fig. 3(b), G_{64} is found to be 0.98, which means that the signals are very similar in shape. Taking benefit of the 128 acquired signals, one can calculate the mean correlation G and the observed standard deviation δG:

$$G=\frac{1}{128}\sum_i G_i, \tag{3a}$$

$$\delta G=\frac{1}{8}\left[\frac{1}{128}\sum_i (G_i-G)^2\right]^{1/2}, \tag{3b}$$

where the $1/8=1/\sqrt{64}$ factor in (3b) accounts for the fact that we consider that our 128 transducers give us 64 uncorrelated measurements. A correction may be applied in order to take into account the possible presence of additive noise (see Appendix A). However, in our experimental conditions, the corrective term was negligible (between 10^{-6} and 10^{-2}).

Before presenting the experimental results, it is worth emphasizing the importance of having 128 receivers for this experiment (which is not limited to estimating the statistical dispersion δG). The sum on the 128 channels that appears in Eq. (1) can be necessary to determine unambiguously the peak of correlation. As an illustration, Fig. 5 presents plots of the correlation $g(t)$ for a temperature decrease of $\Delta T=2$ °C, when a 5-μs time window starting at 300 μs is considered (i.e., 113 μs after the ballistic time). While the sum over the 128 channels gives a clear peak around 2 μs, the correlation is not sufficient to determine the proper time shift when it is performed on a single channel. This is very similar to time-reversal focusing through a multiply scattering slab: a significant focusing peak (in space and in time) can be obtained with a single transducer, provided the time window is large enough compared to the correlation time of the scattered sig-

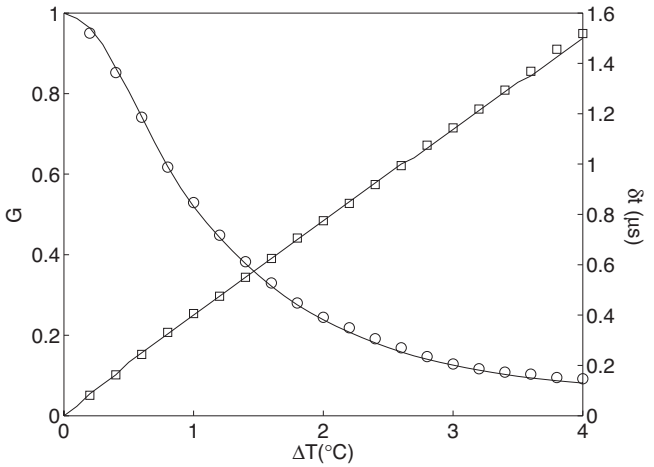

FIG. 6. Experimental results: amplitude of correlation G (circles) and time shift δt (squares) as functions of temperature decrease ΔT for a correlation calculated from the entire coda ($\Delta\tau = 390\ \mu$s). Solid line: prediction of the model.

nals; for smaller time windows, which are required in a time-resolved experiment, it is necessary to use an array and not just a single element to see the focusing peak emerge unambiguously [19,29].

III. EXPERIMENTAL RESULTS AND DISCUSSION

The measurements are performed in the time domain. The incoming signals are short ultrasonic pulses with a central frequency of 3 MHz and the frequency band we consider here is 2.4–4 MHz. To investigate the influence of a slight temperature change ΔT on the multiply scattered signals, we study the impact of ΔT both on the time shift δt and on the amplitude of correlation G. We will particularly focus on three kinds of situation: (A) the beginning time τ is taken at the ballistic time (first arrival) and G is measured as a function of the duration of the time-window $\Delta\tau$; (B) $\Delta\tau$ is fixed to a value much smaller than τ_D, so that the envelope of the coda is constant within that window, and G is measured as a function of τ, the central time of the window; (C) same as (B) except that signals are filtered in narrow frequency bands and G is measured as a function of τ and of the central frequency of the filter.

A. Influence of the time window width

Figure 6 displays the time shift δt and the amplitude of correlation G as functions of the temperature decrease ΔT, when the complete signals are taken for the analysis ($\Delta\tau \to \infty$). As the temperature decreases, the multiply scattered signal undergoes an increasing time delay and its correlation with the reference signal gradually deteriorates. These effects can be well understood and accounted for by a simple "shot-noise" model [19,30]. Ideally, the determination of G would require precise knowledge of the scattered signals, which is of course out of reach. However, as is often the case for treating propagation in multiply scattering media, one can follow a statistical approach. The scattered signal $h(t)$ is considered as one realization of a random process. It is represented as a series of replicas of the incoming pulse $e(t)$ arriving at random times t_n:

$$h(t) = \sum_n e(t - t_n). \tag{4}$$

Time t_n represents the travel time corresponding to the nth scattering path within the sample; t_n and t_p $(n \neq p)$ are assumed to be independent and identically distributed random variables. Although correlations between scatterers may exist [23] and yield a correlation between the arrival times, they are neglected here. The probability density function for the arrival times is denoted $A(t)$. The possible values for t_n may extend from the ballistic time to infinity, but a physical measurement of the typical spreading of $A(t)$ is given by τ_D. The incoming signal $e(t)$ is assumed to contain no continuous component, and its duration is much smaller that the time spreading of the coda. Thus, the statistical average of the scattered signal is

$$\langle h(t)\rangle = \sum_n \int e(t - t_n)A(t_n)dt_n = 0 \tag{5}$$

and its variance is given by:

$$\langle h^2(t)\rangle = \sum_p \sum_{n\neq p} \int\int e(t - t_n)e(t - t_p)A(t_n)A(t_p)dt_n dt_p + \sum_n \int e(t - t_n)^2 A(t_n)dt_n \tag{6}$$

$$= A(t)N_{sp}\int e^2(t)dt, \tag{7}$$

with N_{sp} the total number of scattering paths. For simplicity, we will assume that the incoming signal is normalized so that $\int e^2(t)dt = 1$. Then $A(t)N_{sp}$ can be identified with the time-of-flight distribution for the intensity, $I(t) = \langle h^2(t)\rangle$. Another important statistical parameter is the autocorrelation function of the scattered signal:

$$\langle h(t_1)h(t_2)\rangle = \sum_p \sum_{n\neq p} \int\int e(t_1 - t_n)e(t_2 - t_p)A(t_n)A(t_p)dt_n dt_p + \sum_n \int e(t_1 - t_n)e(t_2 - t_n)A(t_n)dt_n \tag{8}$$

$$= I((t_1 + t_2)/2)r(t_2 - t_1), \tag{9}$$

with $r(t) = e(t) \otimes e(-t) = \int e(\theta)e(t + \theta)d\theta$. The typical correlation time for the scattered wave form is therefore determined by the initial pulse length.

Note that other forms of shot-noise models can be considered. For instance, the decay of the amplitude with the path length ($1/\sqrt{ct_n}$ in two dimensions, $1/ct_n$ in three dimensions) can be incorporated. Alternatively, the arrival times can be assumed to be uniformly distributed and the amplitude associated with each path treated as independent random variables. As a whole, the multiply scattered signal can be con-

sidered as a nonstationary random process with a variance that changes with time. These various approaches yield the same conclusion: $h(t)$ is modeled as a zero-mean nonstationary process with a correlation time determined by the incoming pulse (or equivalently the inverse of the frequency bandwidth) and a variance proportional to the time-of-flight distribution $I(t)$, which shows a characteristic time—e.g., τ_D or τ_{90}. Moreover, if the number of paths arriving at time t is large enough, $h(t)$ can be assumed to have Gaussian statistics (by virtue of the central-limit theorem). This assumption can be useful to evaluate higher-order moments of the scattered signals, if necessary.

When the temperature decreases ($T \to T-\Delta T$), ultrasonic waves propagate more slowly in water ($c \to c-\Delta c$) and the travel time t_n becomes $t_n' = t_n/(1-\Delta c/c) \simeq (1+\Delta c/c)t_n$. For water around 25 °C, we have (in mm/μs) $\Delta c = 2.7 \times 10^{-3}\Delta T + 3.4 \times 10^{-5}\Delta T^2$ [31], so $\Delta c/c = 0.18\%$ for $\Delta T = 1$ °C and $\Delta c/c = 0.76\%$ for $\Delta T = 4$ °C, which is the largest temperature change we will consider here. Following the shot-noise approach, the effect of a temperature change is a change of sound speed which results in a pure time dilation of the arrival times in the scattered signal, the dilation factor being here very close to unity:

$$h^{\Delta T}(t) = \sum_n e(t-t_n') = \sum_n e[t - t_n(1+\Delta c/c)]. \tag{10}$$

The cross correlation between the scattered wave forms before and after the change in temperature reads

$$g(t) = \int h(\theta)h^{\Delta T}(t+\theta)d\theta. \tag{11}$$

Its average value is

$$\begin{aligned}\langle g(t)\rangle &= \int \sum_p \sum_{n\neq p} e(\theta - t_n)e(t+\theta-t_p')A(t_n)A(t_p)dt_n dt_p d\theta \\ &+ \int\int \sum_n e(\theta-t_n)e(t+\theta-t_n')A(t_n)dt_n d\theta \\ &= \int I(\theta)r(t-\theta\Delta c/c)d\theta. \end{aligned} \tag{12}$$

Once the time-of-flight distribution $I(t)$ is estimated from the experimental measurements [see Fig. 2(b)], Eq. (12) can be used to obtain $\langle g(t)\rangle$, giving the prediction of the shot-noise model for the time shift δt and the amplitude of correlation G. Figure 6 shows that the agreement with the experimental measurements is excellent, demonstrating that the shot-noise model picks the main features of the effect of the temperature change on the correlation.

From Eq. (12), it is difficult to give general expressions for δt and G, but approximate results can be obtained in simple cases, which we discuss now.

First, an equivalent expression for Eq. (12) is

$$\langle g(t)\rangle = \frac{c}{\Delta c}\int I\left(\frac{c}{\Delta c}\theta\right)r(\theta - t)d\theta. \tag{13}$$

Since $I(t)$ is maximum at a time τ_M and its typical duration is $\Delta\tau_{90}$, $I\left(\frac{c}{\Delta c}\theta\right)$ takes significant values for $(\tau_M - \Delta\tau_{90}/2)\Delta c/c < \theta < (\tau_M + \Delta\tau_{90}/2)\Delta c/c$. Furthermore, as $r(t)$ is maximum at $t=0$, G should attain its maximum value for a time shift $\delta t \simeq \tau_M \Delta c/c$, even though the precise value of δt depends on the exact shape of $I(t)$. Besides, since the incoming signal $e(t)$ is a pulse with a central frequency $f_0 = \omega_0/2\pi$, $r(t)$ behaves approximately as $\cos(\omega_0 t)$ for $|t| < 1/(4f_0)$ nearly independently from the actual envelope of $e(t)$. When $\Delta\tau_{90}\Delta c/c \ll 1/(2f_0)$, $G \simeq \int I(t)dt = 1$ whereas $G \simeq \int r(t)dt = 0$ for $\Delta\tau_{90}\Delta c/c \gg 1/(2f_0)$. The transition occurs when half a period of the cosine $\cos(\omega_0 t)$ embraces the typical spreading $\Delta\tau_{90}\Delta c/c$: in that case the integral in Eq. (13) will (very) approximately be $(90\% - 10\%) \times 2/\pi \sim 0.5$ since $2/\pi$ is the mean value of the cosine over half a period. This gives the relative change $(\Delta c/c)_{1/2}$ or the temperature change $(\Delta T)_{1/2}$ needed to provoke a significant decorrelation ($G \sim 0.5$) of the scattered signals [32,33]:

$$\left(\frac{\Delta c}{c}\right)_{1/2} \sim \frac{1}{2f_0\Delta\tau_{90}} = 0.14\%, \tag{14}$$

$$(\Delta T)_{1/2} \sim \frac{c}{2f_0\Delta\tau_{90}(\partial c/\partial T)} = 0.77\ ^\circ\mathrm{C}. \tag{15}$$

The orders of magnitude are consistent with the experimental results (Fig. 6). Note that the dimensionless product $Q = \omega_0\Delta\tau_{90}$ (or some other characteristic time for the duration of the coda) is similar to a "coda quality factor" (here, including diffusion and absorption effects). It can serve as an indicator of the sensitivity of the scattering response to a small change: naturally, as Q is enlarged (i.e., strongly scattering medium with little intrinsic absorption), the medium becomes more sensitive to a small perturbation of the sound velocity.

Now, consider the case where the time window of interest $[\tau, \tau+\Delta\tau]$ does not include the whole coda, but begins at a given time (usually the ballistic time) and $\Delta\tau$ is progressively varied. In that case the integral in Eq. (12) runs from τ to $\tau+\Delta\tau$. It has been assumed that $\langle h(t)\rangle = 0$, which is valid if $\Delta\tau$ is larger than the duration of the incoming pulse and if only small time shifts δt are considered. Hence,

$$\langle g(t)\rangle = \int_\tau^{\tau+\Delta\tau} I(\theta)r(t-\theta\Delta c/c)d\theta. \tag{16}$$

For small values of $\Delta\tau$ relatively to the fluctuation time of $I(t)$, it is worth considering the case were $I(t)$ is approximately constant, which yields:

$$\langle g(t)\rangle = \frac{1}{\Delta\tau}\frac{c}{\Delta c}\int_{\tau\Delta c/c}^{(\tau+\Delta\tau)\Delta c/c} r(\theta - t)d\theta, \tag{17}$$

where we renormalized $I(t)$ so that $\int_\tau^{\tau+\Delta\tau} I(\theta)d\theta = 1$. Since $r(t)$ is even and reaches its maximum at $t=0$, the maximum of $\langle g(t)\rangle$ is obtained for the center of the time window:

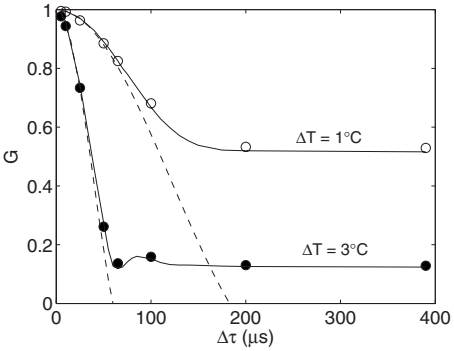

FIG. 7. Experimental results: amplitude of correlation as a function of the time window width for two different temperature decreases: $\Delta T=1$ °C (open circles) and $\Delta T=3$ °C (solid circles). Predictions of the shot-noise model are also shown (solid lines), along with the simple case considered in Eq. (19) (dashed lines).

$$\delta t = \frac{\Delta c}{c}(\tau + \Delta\tau/2), \tag{18a}$$

$$G = \frac{2}{\Delta\tau}\frac{c}{\Delta c}\int_0^{\Delta\tau/2\ \Delta c/c} r(\theta)d\theta. \tag{18b}$$

Once again, since the incoming signal $e(t)$ is a pulse with a central frequency $f_0=\omega_0/2\pi$, $r(t)$ behaves approximately as $\cos(\omega_0 t)$ for $|t|<1/(4f_0)$. Therefore, as long as $\Delta c\ \Delta\tau/2c < 1/(4f_0)$, we obtain

$$G = \mathrm{sinc}\left(\frac{\omega_0\Delta\tau}{2}\frac{\Delta c}{c}\right), \tag{19}$$

where sinc is the sinus cardinalis $[\mathrm{sinc}(x)=\sin(x)/x]$. The condition $\Delta c\ \Delta\tau/2c<1/(4f_0)$ requires that the elongation (or contraction) of the arrival times due to the temperature change must be smaller than a half period. Figures 7 and 8 show that the experimental results are in good agreement with this prediction. Naturally, for large values of $\Delta\tau$, the time-of-flight distribution can no longer be considered as a constant. In that case, G has to be calculated from Eq. (16). As we mentioned earlier, if the coda quality factor is such that $\Delta\tau_{90}\Delta c/c \gg 1/2f_0$, then G will tend to 0 as the time-window is enlarged. This is not always the case, as is shown in Fig. 7: for a given $\Delta c/c$, the coda may not spread long enough (i.e., Q is too small) to reach the regime of full decorrelation ($G=0$). In that case G and δt show a plateau for large values of ΔT.

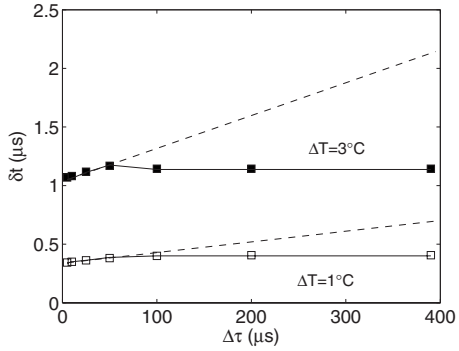

FIG. 8. Experimental results: time shift as a function of the time window width for two different temperature decreases: $\Delta T=1$ °C (open squares) and $\Delta T=3$ °C (solid squares). Predictions of the shot-noise model are also shown (solid lines), along with the simple case considered in Eq. (18a) (dashed lines).

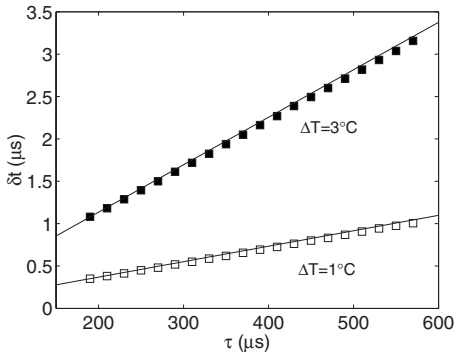

FIG. 9. Analysis with 5-μs time windows for two different ΔT. Influence of arrival time τ on the time shift δt. Solid lines correspond to the shot-noise model [Eq. (18a)].

B. Influence of the time of arrival

It is interesting to note that, in this simple model, the decorrelation brought by the temperature change is not related to any "loss of information." The apparent decorrelation occurs only because the temperature decrease causes a *dilation* of the arrival time, whereas an analysis based on standard correlation functions considers time *translations*. The amplitude of correlation given by Eq. (19) increases as shorter time windows are considered, because the difference between a dilation and a translation is less marked on short windows. Whatever the length of the window, an important prediction of the shot-noise model is that the loss of correlation should not depend on the position of the selected window. The arrival times that lie between τ and $\tau+\Delta\tau$ are stretched into the interval $[\tau+\tau\,\Delta c/c, \tau+\Delta\tau+\tau\,\Delta c/c+\Delta\tau\,\Delta c/c]$, but the elongation of the time window, which is the origin of the decorrelation, is $\Delta\tau\,\Delta c/c$ independently from τ. In other words, there should be no "dynamic effect": for a fixed $\Delta\tau$, G should remain the same whether the window is taken at the beginning of the scattered signals or in the late coda. In order to challenge this idea, let us now consider short windows for our analysis ($\Delta\tau=5$ μs)—so that Eqs. (19) and (18a) are valid expressions—and observe how the correlation changes with the arrival time τ. As already depicted by Fig. 3, the time shift δt increases with τ. Figure 9 shows that this increase is linear and well predicted by Eq. (18a), confirming that the main mechanism for the time delay is indeed a time dilation. On the other hand, Fig. 10 brings a striking piece of evidence that the model is incomplete: experimental data exhibit a stronger decorrelation as one inspects later arrival times. There is indeed a "dynamic effect."

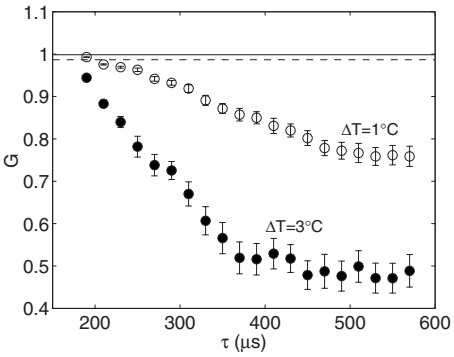

FIG. 10. Analysis with 5-μs time windows for two different ΔT. Influence of arrival time τ on the amplitude of correlation G. Lines correspond to the shot-noise model [Eq. (19)] for $\Delta T=1$ °C (solid line) and $\Delta T=3$ °C (dashed line).

A refined model is thus needed to account for the influence of the arrival time on the decorrelation. The main deficiency of the shot-noise model is to forget about the role of the scatterers on the decorrelation. Indeed, the cumulated phase for a signal traversing the sample does not come only from its propagation through water, but also from all the scatterings it underwent. Consequently, if the behavior of the scatterers is influenced by the temperature, it may have an effect on the correlation. When a monochromatic plane wave $e^{i(k_0 r-\omega t)}$ impinges on a rod, in the far field the scattered wave is cylindrical with an amplitude a depending on the scattering angle θ: $a(\theta)e^{i(k_0 r-\omega t)}/\sqrt{r}$ with r the distance from the scatterer. The differential scattering cross section $\sigma(\theta)=|a(\theta)|^2$ as well as the total scattering cross section $\sigma_T=\int_0^{2\pi}|a(\theta)|^2 d\theta$ are fundamental quantities that determine the elastic and transport mean free paths and the importance of multiply scattering phenomena in a slab. But these parameters do not give information about the phase difference brought by the scattering. For elastic scatterers with a size comparable to the wavelength, resonances may occur. This results in larger phase shifts between the incident and scattered waves, which can be interpreted as a longer "dwell time" for the wave inside the scatterer [24,34,35]. Moreover, this phase shift strongly depends on the scattering angle and should be affected by a change of temperature since the velocities and densities of the ambient medium and of the scatterers vary with temperature. To give some orders of magnitude, Fig. 11 presents some characteristics for the wave scattered by a steel rod (with radius 0.4 mm, $c_L=5.7$ mm/μs, $c_T=3$ mm/μs, density 7.85 kg/liter) in water.

Figure 12 displays a simplified situation to explain how we propose to refine the shot-noise model. Consider two multiply scattered paths, denoted by A and B. Both paths have the same total length Λ and both undergo N scatterings during their traverse of the forest, labeled by their angles $\{\theta_1^A,\ldots,\theta_N^A\}$ and $\{\theta_1^B,\ldots,\theta_N^B\}$, respectively. When the temperature decreases by ΔT, waves follow the same paths, but with a velocity $c-\Delta c$, and each scattering occurs with a slight phase difference $\varphi(\theta,\Delta T)$. As a result, the total phase shifts $\Delta\Phi_A$ and $\Delta\Phi_B$ induced by the temperature change are

$$\Delta\Phi_A=\frac{\Delta c}{c}\frac{\omega\Lambda}{c}+\sum_{i=1}^{N}\varphi(\theta_i^A,\Delta T), \tag{20a}$$

$$\Delta\Phi_B=\frac{\Delta c}{c}\frac{\omega\Lambda}{c}+\sum_{i=1}^{N}\varphi(\theta_i^B,\Delta T). \tag{20b}$$

Previously only the first terms of Eqs. (20a) and (20b), which are proportional to the "geometrical" phase shift $\omega\Lambda/c$, were considered: therefore $\Delta\Phi_A=\Delta\Phi_B$ and the effect of temperature was a pure time dilation. The additional terms in Eqs. (20a) and (20b) take into account the phase sensitivity to temperature of the wave scattered by one rod: paths A and B are now differently affected even though their lengths are the same. The phase associated with each path is not only determined by the path length, but becomes "history dependent" since the additional contribution depends on the successive scattering angles within a path. This is the physical origin of the dynamic effect. We assume that successive scatterings in a path are independent, so the mean value and variance of the total phase-shift distribution are

$$\langle\Delta\Phi\rangle=\frac{\Delta c}{c}\frac{\omega\Lambda}{c}+N\langle\varphi\rangle, \tag{21a}$$

$$\langle(\Delta\Phi-\langle\Delta\Phi\rangle)^2\rangle=N\sigma_\varphi^2, \tag{21b}$$

where $\langle\varphi\rangle$ and σ_φ^2 are the mean and variance of the phase shift induced by the temperature change ΔT for the scattering on one rod. As a consequence, $\langle\varphi\rangle$ has an effect on the time shift δt:

$$\delta t=\frac{\Delta c}{c}\tau+N(\tau)\frac{\langle\varphi\rangle}{\omega}, \tag{22}$$

where τ is now the mean time of the window (i.e., windows are $[\tau-\Delta\tau/2,\tau+\Delta\tau/2]$). Moreover, if the number of scatterings, $N(\tau)$, is large, $\Delta\Phi$ has Gaussian statistics and the amplitude of correlation becomes (see Appendix B)

$$G=\mathrm{sinc}\left[\frac{\Delta c}{c}\frac{\omega\,\Delta\tau}{2}\right]\exp\left[-\frac{N(\tau)}{2}\sigma_\varphi^2\right], \tag{23a}$$

$$\sim\mathrm{sinc}\left[\frac{\Delta c}{c}\frac{\omega\,\Delta\tau}{2}\right]\left[1-\frac{N(\tau)}{2}\sigma_\varphi^2\right]. \tag{23b}$$

The decorrelation is thus related to the variance of the perturbation, which is a typical result for correlation of multiply scattered waves (see, for example, Ref. [4], where the perturbation is a displacement of the scatterers). In the limit of small decorrelation, it can be shown that the result is the same even if the Gaussian assumption is not valid (see Appendix B for a detailed calculation).

Since the number of scatterings grows proportionally to time, G can be expected to decay with τ. The slopes of the experimental data (Fig. 10) yield a characteristic time of 1670 μs for $\Delta T=1$ °C and 400 μs for $\Delta T=3$ °C. In order to test the consistency of this approach, we have to evaluate $N(\tau)$ as well as the angular mean value $\langle\varphi\rangle$ and variance σ_φ^2 of the phase shift $\varphi(\theta)$ undergone by the wave scattered on one rod, due to the temperature change. If we denote by ℓ the average length between two successive scatterings, the number of scatterings can be related to the time of arrival by

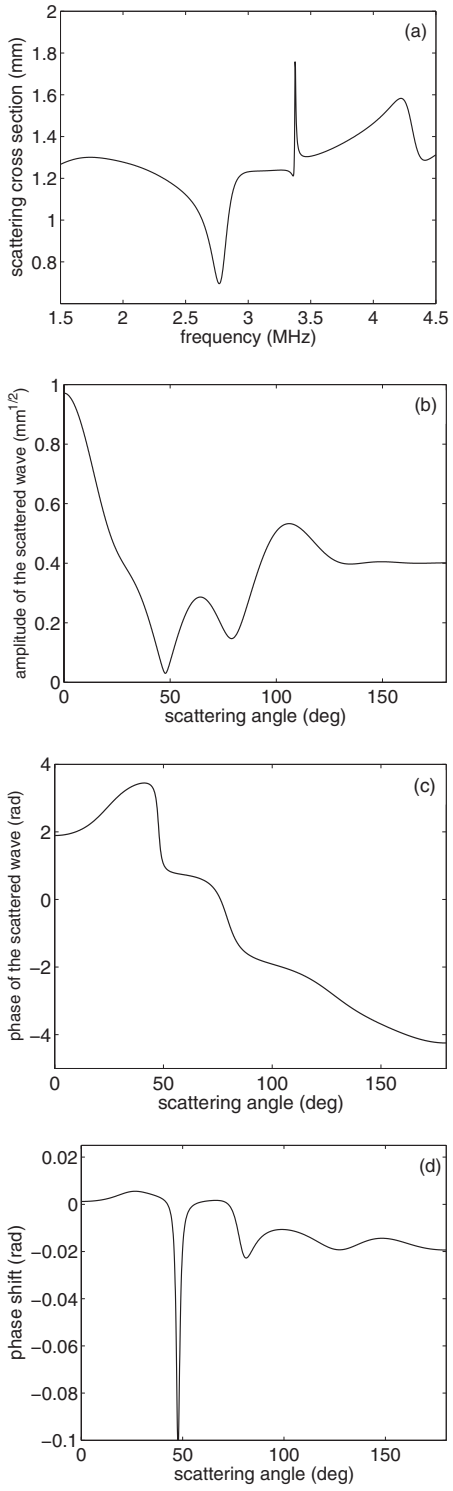

FIG. 11. Scattering properties of a steel rod in water at 25 °C ($c=1.5$ mm/μs). (a) Total scattering cross section versus frequency. Two resonances can be seen at 2.75 MHz and 3.35 MHz, respectively. Note that the first resonance manifests itself as a dip, rather than a peak, because of interferences between the elastic and rigid responses of the rod (see Ref. [24]). (b) Amplitude of the scattered wave at 3 MHz versus the scattering angle θ. (c) Phase of the scattered wave at 3 MHz versus the scattering angle θ. (d) Phase shift undergone by the scattered wave due to a change $\Delta c/c = -0.184\%$ of the sound velocity in water at 3 MHz.

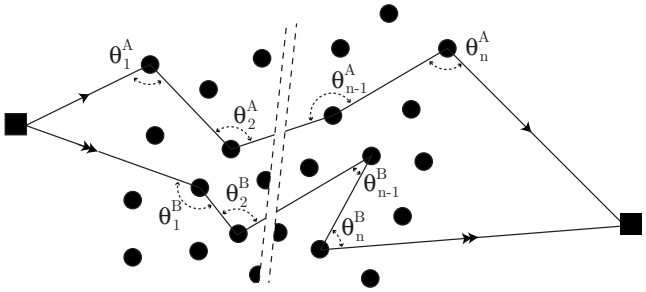

FIG. 12. Example of two paths of N scatterings through the sample with the same total length. Path A is a set of scatterings with angles $\{\theta_1^A, \theta_2^A, \ldots, \theta_N^A\}$, path B with $\{\theta_1^B, \theta_2^B, \ldots, \theta_N^B\}$. From the shot-noise model point of view, both paths are identical, because of the same length. In the refined model, they are discriminated because their set of angles are different.

$$N(\tau) = \frac{L + c(\tau - \tau_0)}{\ell}, \tag{24}$$

where τ_0 is the arrival time of the first pulse (ballistic time) and L the thickness of the sample. We can then introduce ϵ_s and γ_s, the time shift rate and the decorrelation rate due to the scatterers only, respectively defined by

$$\epsilon_s = \left(\frac{\partial(\delta t)}{\partial \tau}\right)_{\Delta c \to 0} = \frac{c\langle\varphi\rangle}{\omega\ell}, \tag{25a}$$

$$\gamma_s = -\left(\frac{\partial G}{\partial \tau}\right)_{\Delta c \to 0} = \frac{c\sigma_\varphi^2}{2\ell}. \tag{25b}$$

In the limit of a small decorrelations, Eqs. (23a) and (23b) thus simplify into

$$\delta t = \left(\frac{\Delta c}{c} + \epsilon_s\right)\tau + \frac{L - c\tau_0}{c}\epsilon_s, \tag{26a}$$

$$\frac{G}{\mathrm{sinc}\left[\frac{\Delta c}{c}\frac{\omega \Delta \tau}{2}\right]} = 1 - \gamma_s\left(\tau - \tau_0 + \frac{L}{c}\right). \tag{26b}$$

Equations (26a) and (26b) provide a good indirect test of the refined model. Indeed, ϵ_s and γ_s can be evaluated in two independent ways, as displayed in Fig. 13. For each ΔT, we calculated the best linear fit to the experimental data for δt as a function of τ, limited to the first 100 μs where the decorrelation remains small. The time shift rate ϵ_s was then calculated independently from the slope of the fitting and from its ordinate at the origin [Fig. 13(a)]. Negative values were found for ϵ_s, indicating that when temperature is decreasing, the rods tend to make the waves traveling faster. For $\Delta T = 1$ °C, for instance, the rate of time shift is roughly equal to -1.3×10^{-4}, which means that the scatterers induce an additional time shift of -1 μs for every 13 000 μs of travel in the sample. This value can be compared with the rate of time shift due to propagation in water, $\Delta c/c$, which is of the order of 1.8×10^{-3} for a 1 °C decrease of temperature. So, in terms of time shift, the effect of the scatterers is about 10 times

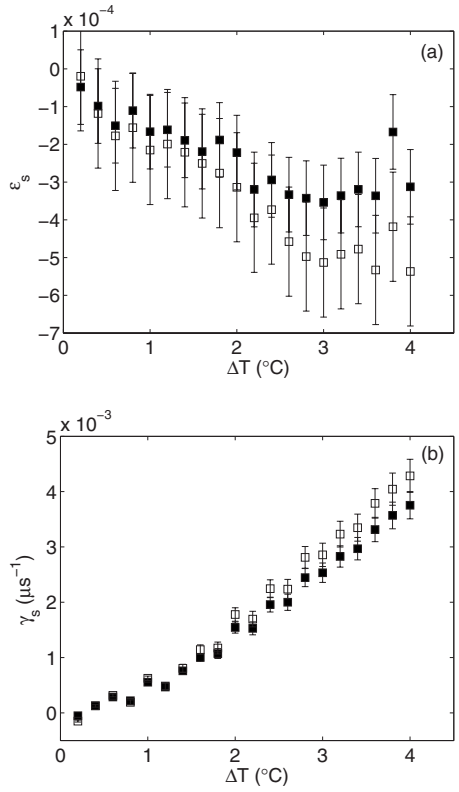

FIG. 13. Test of the refined shot-noise model. For each temperature decrease ΔT, the rate of time shift ϵ_s due to scatterers (a) and the rate of decorrelation γ_s due to scatterers (b) are calculated in two independent ways: from the slope (solid squares) and the ordinate at the origin (open squares) of δt versus τ and G versus τ, respectively. The two estimations are very consistent with each other.

smaller than that of the water, which makes ϵ_s difficult to measure accurately [see Fig. 13(a)].

For the rate of decorrelation, γ_s, the same procedure was followed. The agreement between the two evaluations is excellent, and γ_s is found to increase with ΔT. For $\Delta T=1$ °C, we found $\gamma_s \simeq 0.6\times 10^{-3}$ μs^{-1}. For comparison, the rate of decorrelation due to propagation in water only is zero.

C. Influence of the frequency

In this section, we study the influence of the frequency on γ_s and ϵ_s. To that end, the multiply scattered signals are digitally bandpass filtered. Fifteen 0.2-MHz-wide frequency bands with central frequencies ranging from 2.5 to 3.9 MHz were used. As we mentioned before, the use of an array is particularly important for narrow-band experiments. The duration of the time window is kept small (here $\Delta\tau=10$ μs) in order to achieve time-resolved measurements and still consider that $I(\tau)$ is approximately constant at that scale. Yet because of the smaller frequency bandwidth, the correlation time τ_c of the filtered signals is larger (typically ~ 5 μs). The ability to see the correlation peak emerge is therefore reduced, and it would be impossible to detect it with a single source-receiver pair. Once the signals are filtered, the time

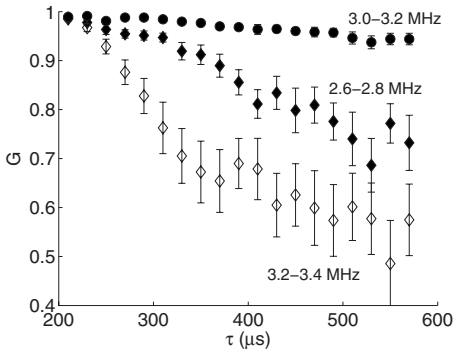

FIG. 14. Amplitude of correlation G as a function of arrival time τ for three different frequency bands: 2.6–2.8 MHz (solid diamonds), 3.0–3.2 MHz (solid circles), and 3.2–3.4 MHz (open diamonds). The temperature difference is $\Delta T=1$ °C, and correlations are calculated on 10-μs time windows.

shift rate ϵ_s and the decorrelation rate γ_s are determined as previously, except that we now have frequency-dependent measurements.

The experimental results clearly point out two frequency bands (around 2.7 and 3.3 MHz) for which the scattering medium exhibits a stronger sensitivity (Fig. 14). Figure 15 presents the experimental results for ϵ_s and γ_s versus frequency. The decorrelation rate γ_s shows a particularly strong frequency dependence, especially around 3.3 MHz. As to the time shift rate ϵ_s, its frequency dependence is less pronounced.

The two frequency bands for which the decorrelation is stronger correspond to resonance frequencies of the scatterers, as can be seen from the plots of the scattering cross section [Fig. 11(a)]. The variations of γ_s with frequency are particularly interesting: the second (and thinnest) of the resonances (around 3.3 MHz) is clearly revealed by the correlation experiment, whereas it could not be detected with a classical spectroscopic measurement of coherent transmission [23,24]. Indeed, experimental measurements of the elastic mean free path ℓ_e did not reveal the second resonance because it is very thin (~ 5 kHz—i.e., 0.15% of the resonance frequency) and its amplitude is not large enough. It would require a very fine frequency resolution, hence a very long recording time and a significant signal-to-noise ratio during that time. This cannot be easily achieved with transmission measurements of the mean free path, because in order to see the coherent wave emerge from experimental measurements, a significant amount of configurational averaging is necessary. From a practical point of view, fluctuations cannot be entirely suppressed, at least not over the time interval needed to see such a thin resonance. In addition to this, the polydispersity of the rod diameters (the ratio of the standard deviation to the mean value is approximately 1.5%) tends to blur out the thinnest resonances.

However, in the coda correlation experiments we discuss here, the relevant parameter is not the *scattering cross section* or the mean free path, but according to the refined model, the *variance of the phase shift* induced by a small temperature change. And this variance happens to be so huge around the second resonance frequency (Fig. 16) that even

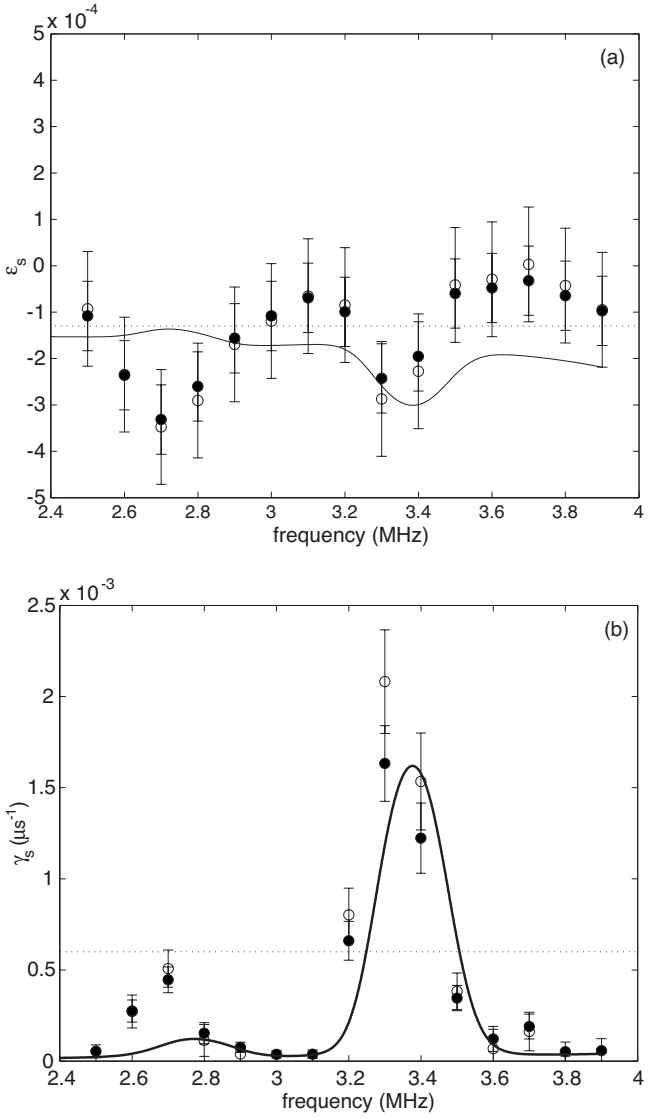

FIG. 15. Variation of the rate of time shift ϵ_s and the rate of decorrelation γ_s as functions of frequency for a temperature decrease of 1 °C. As in Fig. 13, ϵ_s and γ_s are evaluated in two independent ways: from the slope (solid circles) and the ordinate (open circles) of a linear fit. The rate of decorrelation appears to be very sensitive to frequency, and two peaks can be seen. Dashed lines correspond to values found with the whole band of frequency. The solid line shows the prediction for a reasonable model of the behavior of a rod steel with temperature.

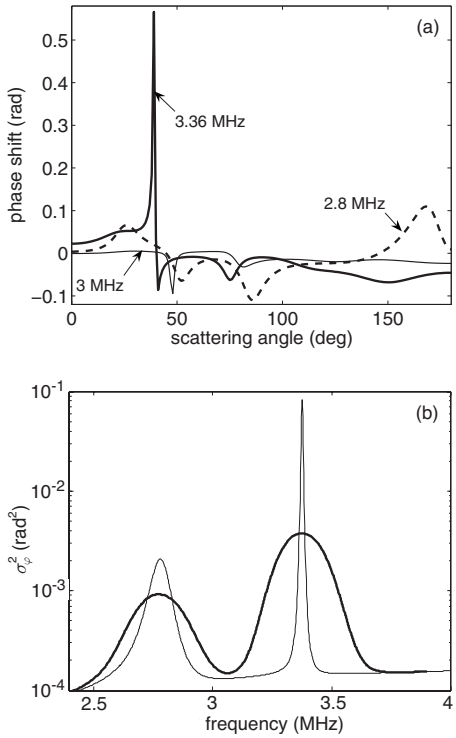

FIG. 16. Calculations for a single rod (radius 0.4 mm, c_L =5.7 mm/μs, c_T=3 mm/μs) when sound velocities in water and steel are changing. (a) The phase shift induced by a change of temperature as a function of the angle of scattering for three different frequencies. (b) Corresponding variance σ_φ^2 versus frequency. In this example, parameters were chosen to simulate a temperature change of 1 °C: $\Delta c/c=-0.184\%$, $\Delta c_L/c_L=5\times10^{-4}$, and $\Delta c_T/c_T=10\times10^{-4}$. The thick curve in (b) takes the effects of the polydispersity and the frequency averaging into account.

though it is partially erased by polydispersity and by the relatively poor frequency resolution, it is far from being entirely washed out: the second resonance even has a stronger impact on γ_s than the first one, which is confirmed by experimental measurements. Because of this effect, a particular resonant frequency of the scatterers that could not be detected from classical measurements of the mean free path is clearly revealed by measuring the dynamic sensitivity of the multiply scattered waves to a very small temperature change.

So far, our indirect test of the refined shot-noise model has allowed us to check the consistency of the mechanisms invoked to explain the decorrelation without any knowledge of the exact scatterer's behavior (i.e., without knowing $\langle\varphi\rangle$, σ_φ, or even ℓ and c). However, from the perspective of using the study of decorrelation as a spectroscopic tool, a more quantitative validation of the model is needed. In other words, can we predict the correct values of γ_s and ϵ_s in a given frequency band? Inversely, what can we say about the scattering medium from experimental measurements of γ_s and ϵ_s? Despite the simplicity of the approximate expressions in Eqs. (25a) and (25b), answering these questions is more difficult than it seems.

To begin with, in order to calculate a theoretical value for γ_s and ϵ_s, $\langle\varphi\rangle$ and σ_φ must be known. We tried to measure the phase variation of the wave scattered by one single rod after a temperature change. Experimentally, these measurements are very difficult, even on a limited domain of scattering angles, first because the biggest contribution to the phase change is due to the change of the sound speed in water [first terms of Eqs. (20a) and (20b)], which has to be subtracted from the total phase. Moreover, the angles for which $\varphi(\theta)$ varies the most are also those for which the amplitude of the scattered wave $|a(\theta)|$ is weak; consequently, the errors bars on the phase measurements were huge (at least 30%), and even though greater variations around 2.7 and 3.3 MHz were observed, the experimental measurements of $\varphi(\theta)$ performed

on a single rod were too imprecise and did not cover all scattering angles. An alternative is to evaluate $\langle\varphi\rangle$ and σ_φ by numerical calculation of the pressure scattered by a steel rod immersed in water [36]. The physical parameters of the rods are the following: its diameter d; its mass density ρ relative to that of water; the velocity of sound in water, c; and the longitudinal and shear velocities of sound in steel, c_L and c_T. How these parameters change with temperature is a tricky question, the answer to which has a strong impact on $\langle\varphi\rangle$ and σ_φ. The effect of the temperature on d and ρ can be crudely estimated and is found to have a negligible impact on the scattering properties of the rod. The temperature dependence of the velocity of sound in water has been widely studied. But the variations with temperature of c_L and c_T in steel are not well known and certainly depend on the way the rods have been manufactured. In the case of aluminum blocks, Weaver and Lobkis [11] reported values of $d(\ln[c_L])/dT=-1.4\times10^{-4}$ K^{-1} and $d(\ln[c_T])/dT=-2.7\times10^{-4}$ K^{-1}. As to steel, the few experimental measurements we found indicate a stronger sensitivity to temperature changes than for aluminum, as well as a strong dependence on the exact composition of the alloy. Typical values lie between -2.5×10^{-4} K^{-1} and -10^{-3} K^{-1}, with a stronger temperature dependence for shear waves [37,38].

Moreover, the relevant wave velocity c in Eqs. (25a) and (25b) and the typical distance ℓ between two scatterings are not unambiguously defined. There are at least three possible ways to evaluate ℓ: the mean distance between two scatterers ($1/\sqrt{n}=2.3$ mm, with $n=18.75$ cm^{-2}), the elastic mean free path ℓ_e, and the transport mean free path ℓ^*. There are also different possible values for the wave speed c: the velocity of sound in water, the phase or group velocity of the effective medium, and the transport velocity. In the literature, the number of scatterings in a path with length ct is often evaluated as ct/ℓ^*. The mean free path ℓ^* is a physical parameter related to the average intensity. It indicates the typical distance after which the energy flux has lost the memory of its initial direction. If ℓ^* was the relevant parameter in our case, then logically the transport speed should be taken as the relevant velocity instead of the velocity of sound in water. Moreover, since at each step with length ℓ^* the memory of the initial direction is lost, the mean and variance of the phase shift should be calculated with the assumption of an isotropic angle distribution: i.e.,

$$\langle\varphi\rangle=\frac{1}{2\pi}\int_0^{2\pi}\varphi(\theta)d\theta, \tag{27a}$$

$$\sigma_\varphi^2=\frac{1}{2\pi}\int_0^{2\pi}(\varphi(\theta)-\langle\varphi\rangle)^2d\theta. \tag{27b}$$

This is in contradiction to the approach we followed (Appendix B), in which the mean and variance of the phase shift take into account the anisotropy of scattering at each step. The elastic mean free path ℓ_e can be taken as a reasonable measure of the distance between two scatterings. In numerical simulations, it is usual to treat diffusive propagation as a random walk with either a fixed step length ℓ_e or an exponential probability distribution for the step length, $P(\ell)=e^{-\ell/\ell_e}/\ell_e$. At each new step, the angle is picked randomly with a probability distribution proportional to the differential scattering cross section [33,39]. This is closer to the approach we followed. By definition, ℓ_e is the extinction length for the ensemble-averaged transmitted wave field: $|\langle\Psi\rangle|^2=\exp(-L/\ell_e)$ for a plane wave traveling a distance L in a lossless scattering medium. The length ℓ_e is related to the coherent wave—i.e., the ensemble-averaged wave. If ℓ_e is chosen as the relevant parameter in our case, the relevant velocity is probably the effective medium velocity, which is also related to the coherent wave, rather than the transport velocity, which is related to the incoherent wave. Depending on the scatterers concentration, both velocities can significantly differ from the ambient medium velocity (here 1.5 mm/μs) in the presence of resonant scattering; in this sample, given the frequency resolution, the velocities do not differ by more than 5% from 1.5 mm/μs.

As an illustration, in Fig. 15 for simplicity we chose to keep $c=1.5$ mm/μs and to take $\ell=\ell_e$ as a measure of the typical distance between two scatterings. The elastic mean free path ℓ_e has been evaluated by Keller's second-order formula [23]. Given the uncertainty in the exact values for $d(\ln[c_{L,T}])/dT$ and the experimental error bars, other choices for ℓ and c can also have given reasonable agreement with the experimental data. Whatever the choice of parameters (within sensible limits) all theoretical calculations show a stronger sensitivity for both resonances, particularly the second one.

Another way to analyze the experimental data is to consider the dimensionless ratio $\beta=\omega\epsilon_s/\gamma_s$. The advantage is that, according to Eqs. (25a) and (25b), β equals $2\langle\varphi\rangle/\sigma_\varphi^2$ and hence depends only on the elastic properties of the rods. Therefore the ambiguity about the relevant choice for the velocity and average distance between scatterings is removed. We can try to fit the experimental values of β with only two adjustable parameters $d(\ln[c_L])/dT$ and $d(\ln[c_T])/dT$. In Fig. 17, we took $d(\ln[c_L])/dT=-5\times10^{-4}$ K^{-1} and $d(\ln[c_T])/dT=-10^{-3}$ K^{-1}. However, except around the second resonance, the experimental errors bars for β are so large that the value of the fit may be questionable. It should also be noted that when the phase shift φ is too strong or varies too abruptly (and this is the case around the second resonance, even for moderate temperature changes), the approximate relations (25a) and (25b) do not hold anymore and more complicated expressions have to be used; this is detailed in Appendix B.

Once reasonable values for $d(\ln[c_L])/dT$ and $d(\ln[c_T])/dT$ are obtained from the study of β, the typical time between two scatterings, $\tau_s=\ell/c$, can be calculated either from ϵ_s [$\tau_s=\langle\varphi\rangle/(\omega\epsilon_s)$] or from γ_s [$\tau_s=\sigma_\varphi^2/(2\gamma_s)$]. As both ϵ_s and γ_s are determined in two independent ways (from the slope and the ordinate at the origin of the linear fit), it gives four independent estimations of τ_s. However, these four estimations appear to be consistent only when the error bars on ϵ_s and γ_s are small enough, which occurs around the resonances (see Fig. 15). We find orders of magnitude for τ_s: between 0.5 and 3 μs in the 2.5–2.8-MHz band and between 1 and 5 μs in the 3.2–3.5-MHz one.

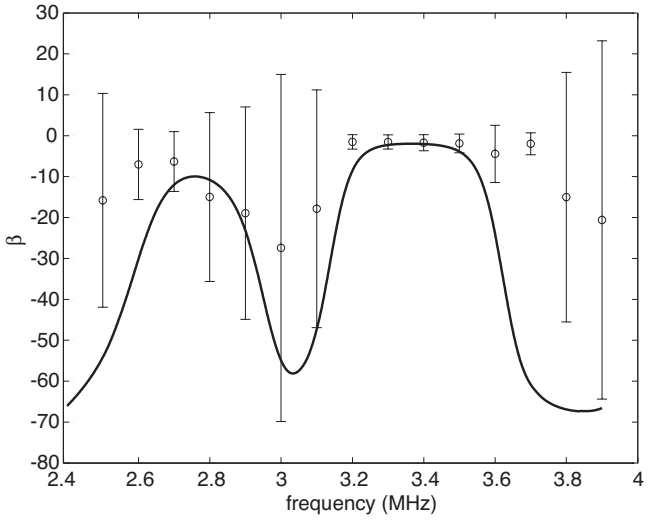

FIG. 17. The dimensionless coefficient $\beta=\omega\epsilon_s/\gamma_s$ is expected to depend only on the elastic properties of the rods, allowing us to estimate $d(\ln[c_L])/dT$ and $d(\ln[c_T])/dT$ independently from the choice made for the distance ℓ between two scatterings and the relevant speed c. The experimental error bars are too large for a precise determination, but $d(\ln[c_L])/dT=-5\times10^{-4}$ K^{-1} and $d(\ln[c_T])/dT=-10^{-3}$ K^{-1} give a reasonable agreement.

IV. CONCLUSION

We have investigated the effect of the temperature on the multiple scattering of ultrasound through a sample of resonant scatterers. By calculating the cross correlation between signals at different temperatures, we followed the evolution of the amplitude of correlation G and of its time shift δt when the temperature was changing.

The main effect of the temperature change, as already observed [3,6,11], is a dilation of the times of arrival due to a change of the velocity of sound, whose impact on the correlation is a linear dependence of δt as a function of the time window position τ (see Fig. 9). Because multiply scattered waves travel in the sample over long times, this effect can be used to monitor the evolution of $\Delta c/c$ with an excellent accuracy. With our particular experiment, for which the sampling frequency was 160 MHz and coda's length was 300 μs, the smallest change in $\Delta c/c$ one can measure is of the order of 2×10^{-5}. It means that a temperature change as low as 0.02 °C can be detected.

The results we present show that small variations in the behavior of the scatterers, due to the temperature change, are also detectable by DAWS and that their effect can be separated from the aforementioned "bulk" effect. We have employed two parameters intrinsic to the sample: the rate of time shift ϵ_s and the rate of decorrelation γ_s, which account for the role of the scatterers in the time shift and the amplitude of correlation, respectively. Moreover, taking benefit of our 128 channels of acquisition, we have been able to investigate the frequency dependence of the cross correlation. The decorrelation (and, to a lesser extent, the time shift) appears to be significantly stronger for two particular bands of frequency, which correspond to resonances of the scatterers. The ability of DAWS to clearly detect the second of these resonances is of particular interest, as the latter is too narrow in frequency to be detected by standard spectroscopy measurements. This better sensitivity of DAWS can be explained by the fact that it relies on correlations, which are mostly affected by phase changes, whereas other techniques are sensitive to the scattering cross section of the scatterers. It so happens that for the second resonance the effect of the slight change in the medium has a much stronger impact on the phase shift of the waves than on their amplitude.

We have also proposed a simple model which relates the decorrelation to the variance of the phase shifts induced by the temperature change. Reasonable agreement between the model and the experimental results was found. In particular, the physics of the model accounts well for the main observation: decorrelation is large when the variance is large. However, the complete inverse problem has not been solved and we cannot extract from the data reliable values of τ_s, $\Delta c_L/c_L$, or $\Delta c_T/c_T$, for example. This method is thus interesting, but suffers from a lack of average (and hence from large error bars) because the disorder of the medium is fixed and it is necessary to work with measurements resolved both in time and in frequency. An improved setup could consist of two arrays of 128 transducers or of a sample offering natural averaging, as a suspension of moving scatterers.

ACKNOWLEDGMENTS

We thank J.H. Page, M. Fink, A. Tourin, V. Mamou, and R.L. Weaver for useful discussions.

APPENDIX A: INFLUENCE OF THE NOISE ON THE CORRELATION

We wish to evaluate the influence of additive noise on the degree of resemblance G between two deterministic signals $f(t)$ and $g(t)$. Ideally we have

$$G=\frac{\int f(t)g(t)dt}{\sqrt{\int f^2(t)dt}\sqrt{\int g^2(t)dt}}. \tag{A1}$$

Suppose the measurements are corrupted by additive and uncorrelated zero-mean noises $n_1(t)$ and $n_2(t)$, with the same power spectral density $N(\omega)$. The statistical average of the numerator is $\langle\int[f(t)+n_1(t)][g(t)+n_2(t)]dt\rangle=\int f(t)g(t)dt$, while at the denominator we have $\langle\int[f(t)+n_1(t)]^2\rangle=\int f^2(t)dt+P_N$ with $P_N=1/2\pi\int N(\omega)d\omega$ the total noise power in the frequency bandwidth $\Delta\omega$. If we assume that the two signals have equal total power $P_S=\int f^2(t)dt=\int g^2(t)dt$, then the effect of additive noise is to lower the true value of G by a factor of $P_S/(P_S+P_N)$.

The perturbations may originate from electronic noise, quantization noise, etc. The power spectral density of the noise may be estimated by a Fourier analysis of the signals recorded before the arrival of the scattered signals. As to P_S, naturally it decays with time. The resulting noise-to-signal ratio P_N/P_S depends on the frequency band and on the time window selected in the coda. For instance, 200 μs after the

ballistic arrival, its highest value is 0.01 (around 2.4 MHz) and between 2.8 MHz and 3.6 MHz it is below 4×10^{-4}. In the very late coda (400 μs after the ballistic arrival) and at the edges of the frequency band (2.4 MHz or 4.2 MHz) it attains 0.1 at most.

APPENDIX B: THE REFINED MODEL

Within the refined model, the Fourier transform of the scattered signal $h(t)$ at the initial temperature is

$$H(\omega) = E(\omega)\sum_n C_n(\omega)e^{-i\omega t_n}, \tag{B1}$$

where $E(\omega)$ is the spectrum of the incident pulse and $C_n(\omega)$ is a complex amplitude specific to each scattering path. When the temperature is changed, we have

$$H'(\omega) = E(\omega)\sum_n C'_n(\omega)e^{-i\omega t'_n}, \tag{B2}$$

with $t'_n = t_n(1+\Delta c/c)$. Previously it was implicitly assumed that $C_n(\omega)$ was real and constant; the refined model will incorporate the effect of successive scatterings on the amplitude and phase of each path and its temperature dependence.

A particular path is characterized by its "geometrical" time of flight t_n and a sequence of scattering angles $\{\theta_1, \theta_2, \ldots, \theta_N\}$. The θ_i and t_n are treated as independent random variables uniformly distributed on $[-\pi, \pi]$ and $[\tau-\Delta\tau/2, \tau+\Delta\tau/2]$, respectively (in the dynamic experiments, $\Delta\tau$ is small enough for the time-of-flight distribution to be constant). Denoting $a(\theta)$ the complex amplitude of the wave scattered by a single rod, we have

$$\langle C_n\rangle = \left[\frac{1}{2\pi}\int a(\theta)d\theta\right]^N, \tag{B3}$$

$$\langle C_n^* C'_n\rangle = \left[\frac{1}{2\pi}\int a^*(\theta)a'(\theta)d\theta\right]^N, \tag{B4}$$

with a' the amplitude of the scattered wave at the new temperature. Assuming that scattering paths p and n ($n\neq p$) are statistically independent yields

$$\langle H^*(\omega)H'(\omega)\rangle = |E(\omega)|^2\sum_n \langle C_n^* C'_n\rangle\langle e^{i\omega t_n \Delta c/c}\rangle. \tag{B5}$$

Upon normalization, in a monochromatic experiment we have

$$\frac{\langle H^*(\omega)H'(\omega)\rangle}{\sqrt{\langle|H(\omega)|^2\rangle\langle|H'(\omega)|^2\rangle}} = \left[\frac{\int a^*(\theta)a'(\theta)d\theta}{\sqrt{\int|a(\theta)|^2d\theta\int|a'(\theta)|^2d\theta}}\right]^N. \tag{B6}$$

Let us introduce $p(\theta) = \sqrt{\sigma(\theta)\sigma'(\theta)}/\sqrt{\sigma_T\sigma'_T}$ with σ_T the total scattering cross section and $\sigma(\theta)$ the differential scattering cross section. Given the orders of magnitude for the velocity perturbation ($\Delta c/c < 0.76\%$), the total scattering cross section σ_T remains practically unchanged when the temperature is decreased and the effect of the velocity change is mostly on the phase rather than on the amplitude of the wave scattered by one rod, so that we may approximate $p(\theta) \simeq \sigma(\theta)/\sigma_T$. Under this approximation, $p(\theta)$ can be interpreted as a probability density function for the scattering angle of a random walker. Getting rid of unnecessary constants we obtain

$$FT[g(t)] = \mathrm{sinc}\left(\frac{\Delta c}{c}\frac{\omega\Delta\tau}{2}\right)\exp\left(-i\omega\frac{\Delta c}{c}\tau\right) \times\left[\int p(\theta)e^{-i\varphi(\theta)}d\theta\right]^N, \tag{B7}$$

with $\varphi(\theta) = -\mathrm{Arg}(a^*a')$ the phase shift undergone by the wave scattered by one rod when the temperature decreases from T to $T-\Delta T$. Compared to the first shot-noise model, the multiplicative term $X^N = [\int p(\theta)e^{-i\varphi}d\theta]^N$ induces a correction both on the time shift and on the correlation amplitude G, and this correction will increase with the scattering order—i.e., with time. The new time shift and correlation amplitude are given, respectively, by

$$\delta t = \frac{\Delta c}{c}\tau - \frac{N\,\mathrm{Arg}(X)}{\omega}, \tag{B8a}$$

$$G = |X|^N\mathrm{sinc}\left(\frac{\Delta c}{c}\frac{\omega\,\Delta\tau}{2}\right). \tag{B8b}$$

For temperature changes small enough so that $e^{-i\varphi}\simeq 1-i\varphi-\varphi^2/2$, the correlations can be expressed as functions of the mean value and variance of φ:

$$\delta t \simeq \frac{\Delta c}{c}\tau + \frac{N\langle\varphi\rangle}{\omega}, \tag{B9a}$$

$$G \simeq \mathrm{sinc}\left(\frac{\Delta c}{c}\frac{\omega\,\Delta\tau}{2}\right)\left(1-\frac{1}{2}\sigma_\varphi^2\right)^N,$$

$$G \simeq \mathrm{sinc}\left(\frac{\Delta c}{c}\frac{\omega\,\Delta\tau}{2}\right)\left(1-\frac{N}{2}\sigma_\varphi^2\right). \tag{B9}$$

Alternatively and independently of $p(\theta)$, if N is large enough to assume that $\Delta\Phi$ has Gaussian statistics, we have $|\langle e^{-i\Delta\Phi}\rangle| \propto e^{-N/2\sigma_\varphi^2}$, which yields the same result for G in the limit of small decorrelation ($N\sigma_\varphi^2 \ll 1$).

Actually the distribution of scattering angles $p(\theta)$ and the variance σ_φ^2 strongly depend on frequency, particularly around the resonances, and the experiments are not really monochromatic. In the time domain, the correlation $\langle g(t)\rangle$ can be obtained via an inverse Fourier transform:

$$\langle g(t)\rangle = \frac{1}{\Delta\omega}\int_{\omega-\Delta\omega/2}^{\omega+\Delta\omega/2} d\omega\,\mathrm{sinc}\left(\frac{\Delta c}{c}\frac{\omega\Delta\tau}{2}\right) \times\exp\left[-i\omega\left(\frac{\Delta c}{c}\tau - t\right)\right]X^N(\omega). \tag{B10}$$

For small values of $\Delta\omega$ or of $\Delta c/c$, the additional delay

$N\,\mathrm{Arg}(X)/\omega$ may be reasonably constant in the frequency band [in practice, this condition is fulfilled for the data presented in this article, except around the second resonance of the rods, for which the complete (B10) was used]. If such is the case, the maximum value of $\langle g(t)\rangle$ will be given by

$$G = \frac{1}{\Delta\omega}\int_{\omega-\Delta\omega/2}^{\omega+\Delta\omega/2} d\omega\ \mathrm{sinc}\left(\frac{\Delta c}{c}\frac{\omega\Delta\tau}{2}\right)|X(\omega)|^N. \quad \text{(B11)}$$

For the "dynamic" experiments, we took $\Delta\tau=5$ μs or 10 μs. Given the orders of magnitude for $\Delta c/c$ and the maximum frequency band (2.4–4 MHz), the sinc function may be taken out of the integral and replaced by its value at the central frequency. In the limit of small temperature changes we have

$$G = \mathrm{sinc}\left(\frac{\Delta c}{c}\frac{\omega\Delta\tau}{2}\right)\left(1 - \frac{N}{2}\frac{1}{\Delta\omega}\int_{\omega-\Delta\omega/2}^{\omega+\Delta\omega/2}\sigma_\varphi^2 d\omega\right). \quad \text{(B12)}$$

So, under the previous approximations, in a wideband experiment the important parameter for the loss of correlation is the frequency-averaged variance of the temperature-induced phase shift undergone by the wave scattered by one rod.

[1] G. Maret and P. Wolf, Z. Phys. B: Condens. Matter **65**, 409 (1987).
[2] D. J. Pine, D. A. Weitz, P. M. Chaikin, and E. Herbolzheimer, Phys. Rev. Lett. **60**, 1134 (1988).
[3] R. Snieder, A. Grêt, H. Douma, and J. Scaled, Science **295**, 2253 (2002).
[4] R. Snieder and J. H. Page, Phys. Today **60**(5), 49 (2007).
[5] A. Grêt, R. Snieder, and J. Scales, J. Geophys. Res. **111**, B03305 (2006).
[6] P. Roberts, W. Phillips, and M. Fehler, J. Acoust. Soc. Am. **91**, 3291 (1992).
[7] G. Poupinet, W. Ellsworth, and J. Fréchet, J. Geophys. Res. **89**, 5719 (1984).
[8] J. Page, M. Cowan, and D. Weitz, Physica B **279**, 130 (2000).
[9] M. L. Cowan, I. P. Jones, J. H. Page, and D. A. Weitz, Phys. Rev. E **65**, 066605 (2002).
[10] J. Page, M. Cowan, P. Sheng, and D. Weitz, in *Proceedings of the IUTAM Symposium 99/4: Mechanical and Electromagnetic Waves in Structured Media*, edited by R. McPhedran, L. Botten, and N. Nicorovici (Kluwer Academic, Boston, 2001).
[11] R. L. Weaver and O. I. Lobkis, Ultrasonics **38**, 491 (2000).
[12] R. L. Weaver and O. Lobkis, in *Review of Progress in Quantitative Nondestructive Evaluation*, edited by D. Thompson-,Dale Chimentier, and L. Poore (AIP, Melville, NY, 2001), pp. 1480–1486, Vol. 3.
[13] O. I. Lobkis and R. L. Weaver, Phys. Rev. Lett. **90**, 254302 (2003).
[14] A. Derode, A. Tourin, and M. Fink, in *Proceedings of the World Congress on Ultrasonics 2003*, edited by D. Cassereau,M. Deschamps,P. Laugier, and A.Zarembowitch (Société Francáise de Acoustique, Paris, 2003), pp. 851–853.
[15] G. Lerosey, J. de Rosny, A. Tourin, A. Derode, and M. Fink, Appl. Phys. Lett. **88**, 154101 (2006).
[16] A. Derode, A. Tourin, J. de Rosny, M. Tanter, S. Yon, and M. Fink, Phys. Rev. Lett. **90**, 014301 (2003).
[17] G. F. Edelmann, T. Akal, W. S. Hodgkiss, S. Kim, W. A. Kuperman, and H.-C. Song, IEEE J. Ocean. Eng. **27**, 602 (2002).
[18] A. Tourin, A. Derode, and M. Fink, Phys. Rev. Lett. **87**, 274301 (2001).
[19] A. Derode, A. Tourin, and M. Fink, J. Acoust. Soc. Am. **107**, 2987 (2000).
[20] G. Lerosey, J. de Rosny, A. Tourin, A. Derode, G. Montaldo, and M. Fink, Phys. Rev. Lett. **92**, 193904 (2004).
[21] F. M. Cucchietti, H. M. Pastawski, and D. A. Wisniacki, Phys. Rev. E **65**, 045206 (2002).
[22] J. de Rosny, J. H. Page, P. Roux, and M. Fink, Phys. Rev. Lett. **90**, 094302 (2003).
[23] A. Derode, V. Mamou, and A. Tourin, Phys. Rev. E **74**, 036606 (2006).
[24] A. Derode, A. Tourin, and M. Fink, Phys. Rev. E **64**, 036605 (2001).
[25] J. H. Page, H. P. Schriemer, A. E. Bailey, and D. A. Weitz, Phys. Rev. E **52**, 3106 (1995).
[26] P. Sheng, *Scattering and Localization of Classical Waves in Random Media* (World Scientific, Singapore, 1990).
[27] A. A. Chabanov, Z. Q. Zhang, and A. Z. Genack, Phys. Rev. Lett. **90**, 203903 (2003).
[28] J. C. J. Paasschens, Phys. Rev. E **56**, 1135 (1997).
[29] A. Derode, A. Tourin, and M. Fink, Phys. Rev. E **64**, 036606 (2001).
[30] A. Derode, A. Tourin, and M. Fink, J. Appl. Phys. **85**, 6343 (1999).
[31] H. J. McSkimin, J. Acoust. Soc. Am. **37**, 325 (1965).
[32] L. E. Ballentine and J. P. Zibin, Phys. Rev. A **54**, 3813 (1996).
[33] R. K. Snieder and J. A. Scales, Phys. Rev. E **58**, 5668 (1998).
[34] H. P. Schriemer, M. L. Cowan, J. H. Page, P. Sheng, Z. Liu, and D. A. Weitz, Phys. Rev. Lett. **79**, 3166 (1997).
[35] A. Lagendijk and B. A. V. Tiggelen, Phys. Rep. **270**, 143 (1996).
[36] L. Flax, G. Gaunaurd, and H. Überall, *Physical Acoustics* (Academic Press, New York, 1981), Vol. XV.
[37] B. Latella and S. Humphries, Scr. Mater. **51**, 635 (2004).
[38] A. Focke, *Metals Handbook*, 9th ed. (ASM International, Metals Park, OH 1990), Vol. 1.
[39] L. Margerin, M. Campillo, and B. A. V. Tiggelen, Geophys. J. Int. **145**, 593 (2001).